



Novel Hierarchical Fe(III)-Doped Cu-MOFs With Enhanced Adsorption of Benzene Vapor

Xuejiao Sun¹, Xiulian Gu¹, Wentao Xu¹, Wen-Jie Chen¹, Qibin Xia^{2*}, Xiaoyang Pan¹, Xiaojing Zhao¹, Yi Li³ and Qi-Hui Wu^{4*}

¹ School of Chemical Engineering and Materials Science, Quanzhou Normal University, Quanzhou, China, ² School of Chemistry and Chemical Engineering, South China University of Technology, Guangzhou, China, ³ Jiangsu Key Laboratory of Advanced Functional Polymer Design and Application, Department of Polymer Science and Engineering, College of Chemistry, Chemical Engineering and Materials Science, Soochow University, Suzhou, China, ⁴ College of Mechanical and Energy Engineering, Jimei University, Xiamen, China

OPEN ACCESS

Edited by:

Qiang Wang,
Beijing Forestry University, China

Reviewed by:

Takashi Okubo,
Kindai University, Japan
Linhai Duan,
Guangdong University of
Petrochemical Technology, China

*Correspondence:

Qibin Xia
qbxia@scut.edu.cn
Qi-Hui Wu
qihui_wu@xmu.edu.cn

Specialty section:

This article was submitted to
Inorganic Chemistry,
a section of the journal
Frontiers in Chemistry

Received: 16 June 2019

Accepted: 11 September 2019

Published: 27 September 2019

Citation:

Sun X, Gu X, Xu W, Chen W-J, Xia Q,
Pan X, Zhao X, Li Y and Wu Q-H
(2019) Novel Hierarchical Fe(III)-Doped
Cu-MOFs With Enhanced Adsorption
of Benzene Vapor.
Front. Chem. 7:652.
doi: 10.3389/fchem.2019.00652

New hierarchical Fe(III)-doped Cu-MOFs (Fe-HK) were developed via introduction of Fe³⁺ ions during HKUST-1 synthesis. The obtained products were characterized by N₂ adsorption, X-ray diffraction, scanning electron microscopy, energy dispersive spectroscopy, FTIR spectroscopy, and thermal analysis. The adsorption isotherms and kinetics of benzene vapor were measured and consecutive adsorption–desorption cycles were performed. It was found that the hierarchical-pore Fe-HK-2 exhibited optimal textural properties with high BET surface area of 1,707 m²/g and total pore volume of 0.93 cm³/g, which were higher than those of the unmodified HKUST-1. Significantly, the hierarchical-pore Fe-HK-2 possessed outstanding benzene adsorption capacity, which was 1.5 times greater than the value on HKUST-1. Benzene diffusivity of Fe-HK-2 was 1.7 times faster than that of parent HKUST-1. Furthermore, the benzene adsorption on Fe-HK-2 was highly reversible. The hierarchical-pore Fe-HK-2 with high porosity, outstanding adsorption capacity, enhanced diffusion rate, and excellent reversibility might be an attractive candidate for VOCs adsorption. This may offer a simple and effective strategy to synthesize hierarchical-pore MOFs by doping with other metal ions.

Keywords: HKUST-1, hierarchical-pore, adsorption, benzene, VOC

INTRODUCTION

Volatile organic compounds (VOCs) as hazardous air pollutants are the precursors of ozone and smog (Zhang et al., 2019). They are derived from various industrial processes and applications of chemical products. The emissions of VOCs have caused severe environmental and healthy issues causing cancer and death (Zhu et al., 2016, 2019; Meng et al., 2019). Therefore, the reduction of VOCs emissions is of great significance. Adsorption with appropriate materials as VOC adsorbent has been known as an energy-efficient and promising strategy (Vellingiri et al., 2017; Zhang et al., 2017; Sui et al., 2019).

Metal-organic frameworks (MOFs), as novel adsorbents, have been attracted considerable attention owing to their excellent specific surface and porosity, as well as tunable topologies (Sun et al., 2014; Ahmed and Jhung, 2016; Li et al., 2018; Lin et al., 2018). Importantly, MOFs have been developed as attractive candidates for VOCs adsorption (Duan et al., 2013; Vellingiri et al., 2016, 2017; Wang et al., 2018). Hu et al. (2018) reported that UiO-66 had the high adsorption capacities of chlorobenzene (4.94 mmol/g) and acetaldehyde (9.42 mmol/g). Xian et al. (2015) indicated that the uptakes of 1,2-dichloroethane and ethyl acetate (EA) on MIL-101(Cr) were separately 9.71 and 5.79 mmol/g. Previously, our results also implied that: (1) MIL-101(Cr) exhibited excellent uptakes of a series of aromatics and *n*-alkanes (7.2–16.3 mmol/g) (Sun et al., 2014, 2017); and (2) MOF-5 possessed high uptakes of linear alkanes *n*C₄–*n*C₇ (8.0–11.5 mmol/g) (Lv et al., 2017). However, most MOFs (e.g., UiO-66, HKUST-1, MOF-5) are microporous with pore sizes <20 Å, which does not benefit molecule diffusion and mass transport (Huang et al., 2015; Yang et al., 2018), inhibiting their applications in VOCs adsorption separation.

Recently, hierarchical-pore MOFs (H-MOFs) are attracting wide attention because of their exceptional properties, including that the micropores can facilitate high surface area, and the mesopores or macropores can enhance molecule diffusion and mass transport (Duan et al., 2018a). Various strategies have been developed to prepare hierarchical porous MOFs, including ligand extension method, mixed ligands method, post-modification method, and template method (Bradshaw et al., 2014; He et al., 2016; Yuan et al., 2017; Chen et al., 2019). Whereas, most of these methods need rigorous experimental conditions and complicated post-treatments (Yang et al., 2018). Moreover, these strategies are disrupted by other disadvantages, such as the high cost of larger ligands, the random copolymerization of mixed ligands, the interpenetrated structures, the collapse of framework after template removal and so on (Yuan et al., 2017; Duan et al., 2018b). Therefore, it is imperative to develop a new strategy to synthesize H-MOFs with high VOCs adsorption capacities.

Notably, HKUST-1 (Cu-BTC) is a potential adsorbent for VOCs due to its high porosity, accessible unsaturated metallic sites, good thermal stability, and easy production (Sun et al., 2015; Wu et al., 2015; Vellingiri et al., 2016). HKUST-1 contains 3D intersectional pores with a window size of 6.0 Å and cage size of 9.0 Å (Zhao et al., 2015). These micropores can offer strong adsorption affinity toward VOCs molecules, but limit their diffusion rate, especially for large ones. Recently, Duan et al. prepared hierarchical-pore HKUST-1 by employing organic amines or dual-functional surfactant as template and investigated its catalytic activity (Duan et al., 2018b,c). Nevertheless, the hierarchical-pore HKUST-1 exhibited lower BET surface area (584–1,241 m²/g) compared to the parent HKUST-1 (1,425 m²/g). Mao et al. (2015) developed a ligand-assisted etching process to prepare the hierarchical porous HKUST-1 with BET surface area of 1,462 m²/g, which showed the enhanced CO₂ adsorption capacity and improved diffusion rate. Chuah et al. (2017) synthesized hierarchically structured HKUST-1 nanocrystals with BET surface area of 1,328 m²/g to improve the SF₆ uptake and adsorption kinetics. However, these approaches are still

complicated and BET surface areas of the hierarchical-pore HKUST-1 need to be further improved. Thus, it is imperative to develop a facile approach to synthesize hierarchical-pore HKUST-1 with high BET surface area and enhanced VOCs adsorption capacity.

In this work, we initiated a simple and effective method to synthesize hierarchical-pore HKUST-1 by introducing Fe³⁺ ions in the HKUST-1 synthesis process. The obtained hierarchical-pore products were characterized, and subsequently their benzene adsorption isotherms and kinetics were measured. Consecutive adsorption–desorption cycles were performed to evaluate the reversibility of benzene adsorption. Importantly, hierarchical-pore HKUST-1 exhibited high porosities with micropores and mesopores. In a result, the hierarchical-pore HKUST-1 showed outstanding benzene adsorption capacities, enhanced diffusion rate and excellent reversibility. Current work indicated that the hierarchical-pore HKUST-1 might be an attractive candidate for VOCs adsorption applications.

EXPERIMENTAL

Materials

Copper nitrate trihydrate [Cu(NO₃)₂·3H₂O, 99%], ferric trichloride hexahydrate (FeCl₃·6H₂O, 99%), and N,N-dimethylformamide (DMF, 99.5%) were purchased from Shanghai Macklin Biochemical Co., Ltd. Benzenetricarboxylic acid (H₃BTC, 99%) was provided from Beijing J&K Chemical Technology Co., Ltd.

Synthesis of Fe-Doped HKUST-1

HKUST-1 was prepared according to the previous report with some modifications (Duan et al., 2018b). In general, copper nitrate trihydrate (1.45 g, 6 mmol) and H₃BTC (0.84 g, 4 mmol) were dissolved in 36 mL DMF. The mixture was then transferred to a Teflon-lined autoclave and heated at 383 K for 21 h. The products were filtered and sequentially washed with DMF and ethanol. Fe-doped HKUST-1 (Fe-HK) samples with different

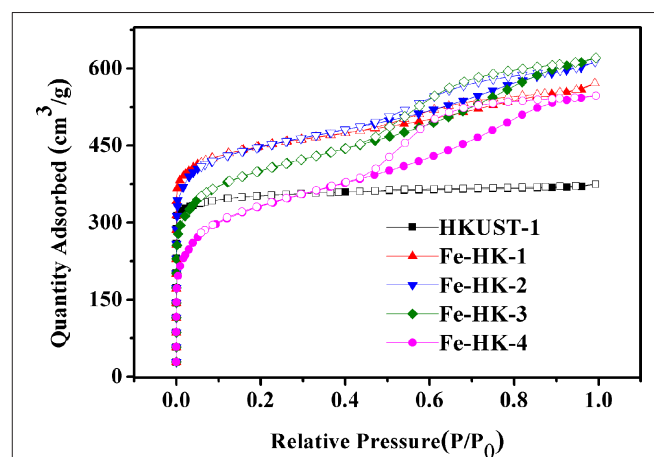


FIGURE 1 | N₂ isotherms of HKUST-1 and Fe-HK series samples at 77 K.

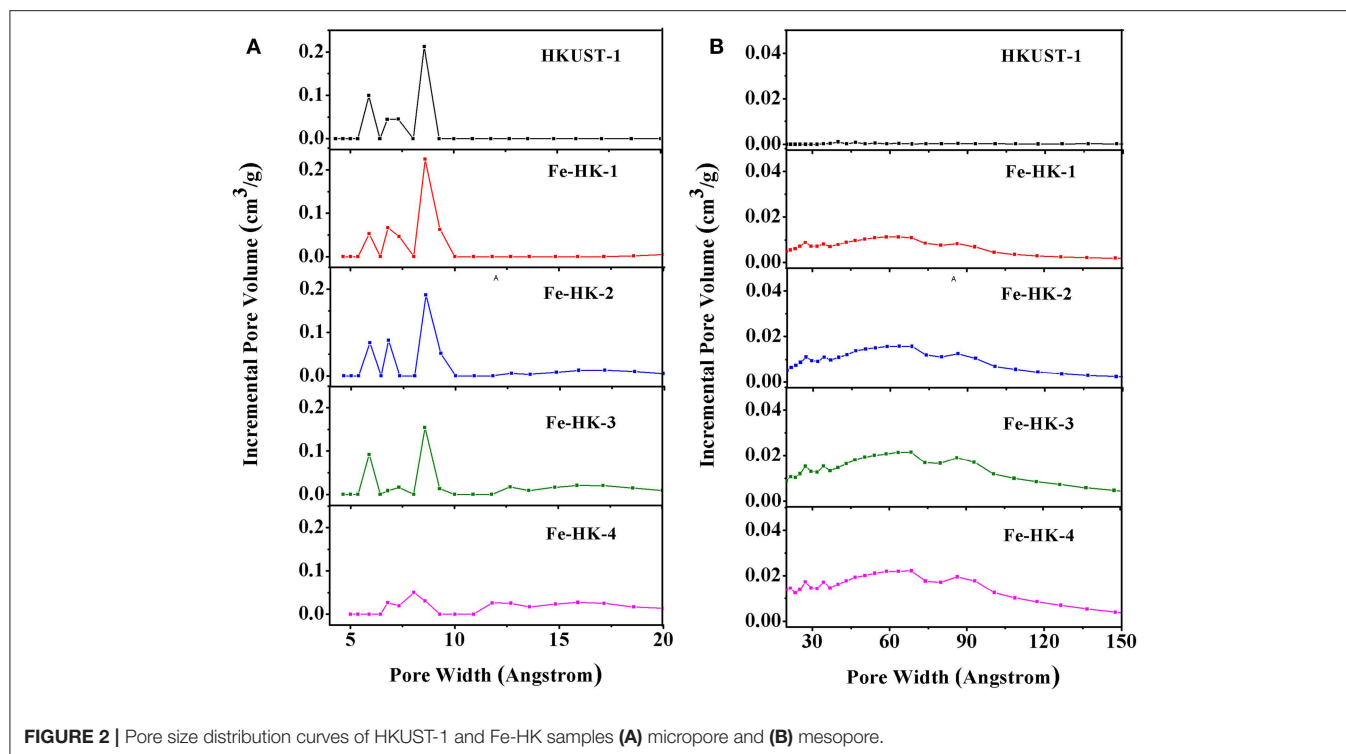


FIGURE 2 | Pore size distribution curves of HKUST-1 and Fe-HK samples (A) micropore and (B) mesopore.

TABLE 1 | Pore structure parameters of HKUST-1 and Fe-HK samples.

Sample	Surface Area (m ² /g)	Pore Volume (cm ³ /g)		
	BET	Total	Micropore	Mesopore
HKUST-1	1400	0.56	0.48	0.08
Fe-HK-1	1729	0.86	0.64	0.22
Fe-HK-2	1707	0.93	0.62	0.31
Fe-HK-3	1495	0.95	0.53	0.42
Fe-HK-4	1226	0.84	0.41	0.43

Fe³⁺/Cu²⁺ molar ratios were synthesized following the similar procedure of HKUST-1, in which the total mole value (6 mmol) of Fe³⁺ and Cu²⁺ was constant by substitution of copper nitrate trihydrate with ferric trichloride hexahydrate. Herein, Fe-HK samples were synthesized with initial Fe³⁺/Cu²⁺ molar ratios of 0.15, 0.20, 0.33, and 0.50, and labeled as Fe-HK-1, Fe-HK-2, Fe-HK-3, and Fe-HK-4, respectively.

RESULTS AND DISCUSSION

Physical Characteristics

Figure 1 shows the N₂ isotherms of HKUST-1 and four Fe-HK samples at 77 K. The isotherm of HKUST-1 exhibits the typical type-I characteristic, indicating the existence of micropores. Whereas, all the Fe-HK samples exhibit typical type-IV isotherms with apparent hysteresis loops, implying the presence of mesopores. These results are further confirmed

by NLDFT pore-size distribution curves of these materials. As shown in Figure 2, HKUST-1 only presents micropores below 10 Å. The pore size below 10 Å is also observed in all Fe-HK samples, suggesting that the porous structure of HKUST-1 is remained in the Fe-HK samples. Comparing to HKUST-1, there are also new micropores (10–20 Å) and mesopores in Fe-HK samples. On one hand, the coordination between Fe³⁺ and carboxylic groups in the BTC can form new micropores and smaller mesopores. On the other hand, Fe³⁺ ions can coordinate with BTC ligand and compete with Cu²⁺ ions to result in the formation of defects and larger mesopores (Horcajada et al., 2014; Zhou et al., 2016). Moreover, the volumes of mesopores increase with Fe³⁺ contents in the Fe-HK samples. These results indicate that Fe-HK samples exhibit hierarchical porous structures.

Table 1 lists the textural properties of HKUST-1 and the Fe-HK samples. Fe-HK-1-3 samples possess higher BET surface areas, micropore volumes and mesopore volumes than HKUST-1, suggesting that the small addition of Fe³⁺ can enhance the porosities of Fe-HK samples. This may be ascribed to the formation of new microporous and mesoporous structures owing to the introduction of Fe³⁺ (Horcajada et al., 2014; Zhou et al., 2016). Additionally, with the increase of molar ratio of Fe³⁺/Cu²⁺ from 0.15 to 0.33, the BET surface areas and micropore volumes of the three Fe-HK samples (Fe-HK-1-3) gradually decrease from 1,729 to 1,495 m²/g and 0.64–0.53 cm³/g, respectively. In contrast, the total pore volumes, mesopore volumes of the three samples increase with the molar ratio of Fe³⁺/Cu²⁺, and could separately reach 0.95 and 0.42 cm³/g. However, Fe-HK-4 (Fe³⁺/Cu²⁺ = 0.5) shows lower BET surface area than HKUST-1, which is possibly attributed to the formation

of the serious crystal defects owing to the excess Fe^{3+} (Zhou et al., 2016). After comprehensive consideration, Fe-HK-2 ($\text{Fe}^{3+}/\text{Cu}^{2+} = 0.20$) was chosen as the optimal sample, which presents BET surface area of $1,707 \text{ m}^2/\text{g}$ and total pore volume of $0.93 \text{ cm}^3/\text{g}$, higher than the previously reported values for hierarchical-pore HKUST-1 prepared with different methods (Mao et al., 2015; Duan et al., 2018b,c).

Figure 3 shows the PXRD patterns of HKUST-1 and the Fe-HK samples. The PXRD patterns of Fe-HK-1-3 samples

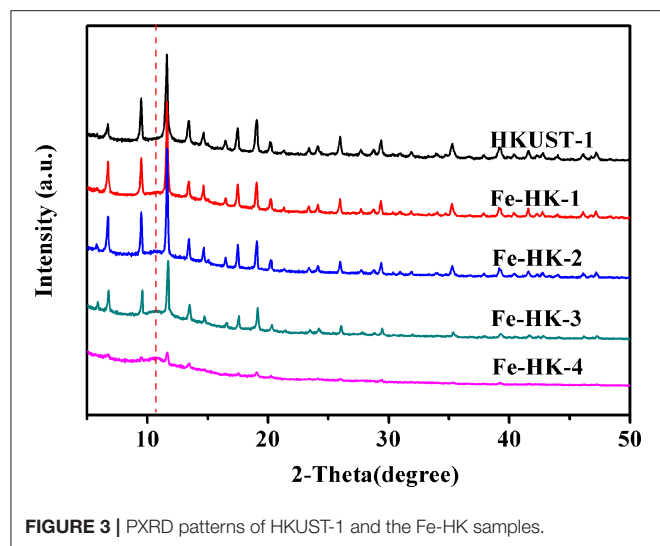
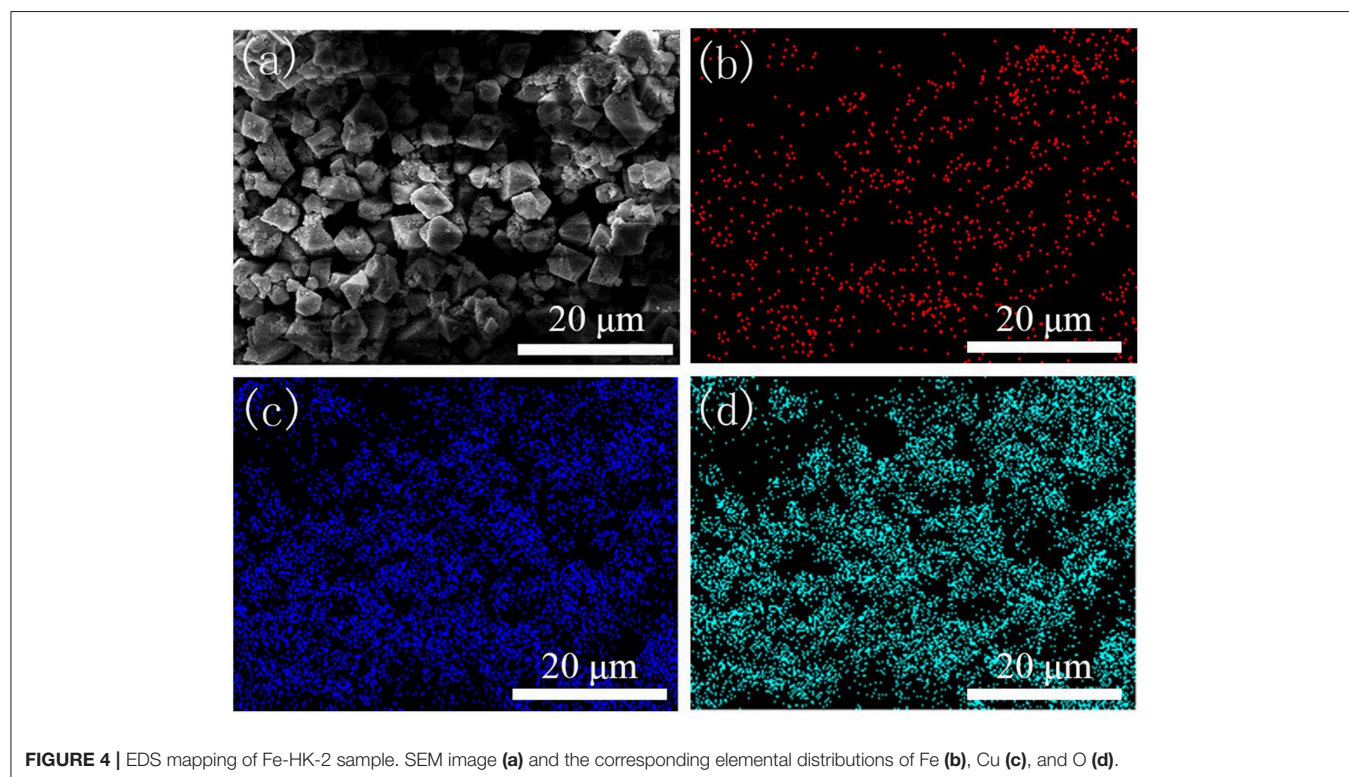
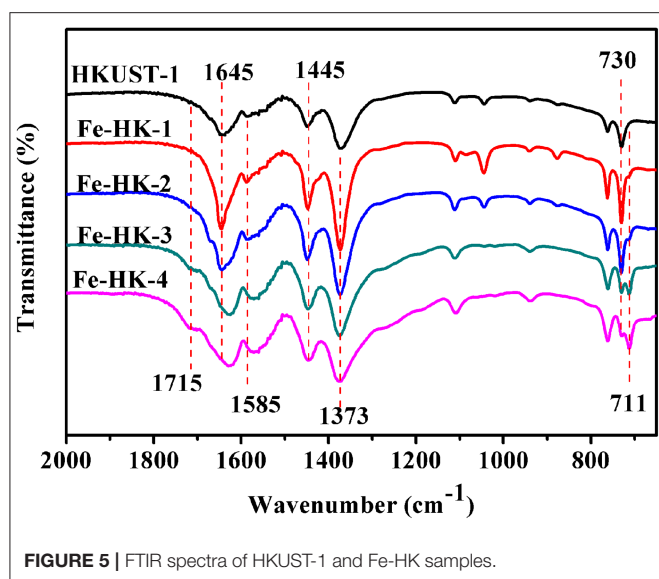


exhibit the main characteristic peaks at 9.4° , 11.6° , 17.5° , and 19.1° , which are identical to that of HKUST-1. It indicates that the Fe-HK-1-3 samples preserve the crystalline characters of HKUST-1, whereas, Fe-HK-4 shows very weak characteristic peaks of HKUST-1 and a new characteristic peak at 10.7° appears. It suggests that when the Fe^{3+} content is higher than certain number, the growth of the HKUST-1 structure would be prevented (Ebrahim and Bandosz, 2013; Zhou et al., 2016). This conclusion is in agreement with the above BET results. Additionally, the new peak at 10.7° may be due to the interaction between Fe^{3+} and carboxylic groups in the BTC.

SEM images of HKUST-1 and the Fe-HK samples are presented in **Figure S1**. It indicates that HKUST-1 has octahedral morphology. The Fe-HK-1-3 samples maintain octahedral structure and their surfaces become rough due to the incorporation of Fe^{3+} . Similar results were also found for other metal ion doping MOFs (Ebrahim and Bandosz, 2013). EDS mapping of the Fe-HK-2 sample was selected as a representative to verify the existence and dispersion of iron ions. As shown in **Figure 4**, the existence of Fe element is clearly confirmed. It is also observed that the Fe and Cu elements are well-dispersed in the Fe-HK-2 crystals, indicating that the iron ions were incorporated successfully into the HKUST-1 framework. The EDS results of Fe/Cu atomic ratios for all Fe-HK samples are listed in **Table S1**. It indicates that the atomic ratios of Fe/Cu in Fe-HK-1, Fe-HK-2, Fe-HK-3 and Fe-HK-4 are 0.17, 0.21, 0.31, and 0.53, respectively, which are very close to their design values.

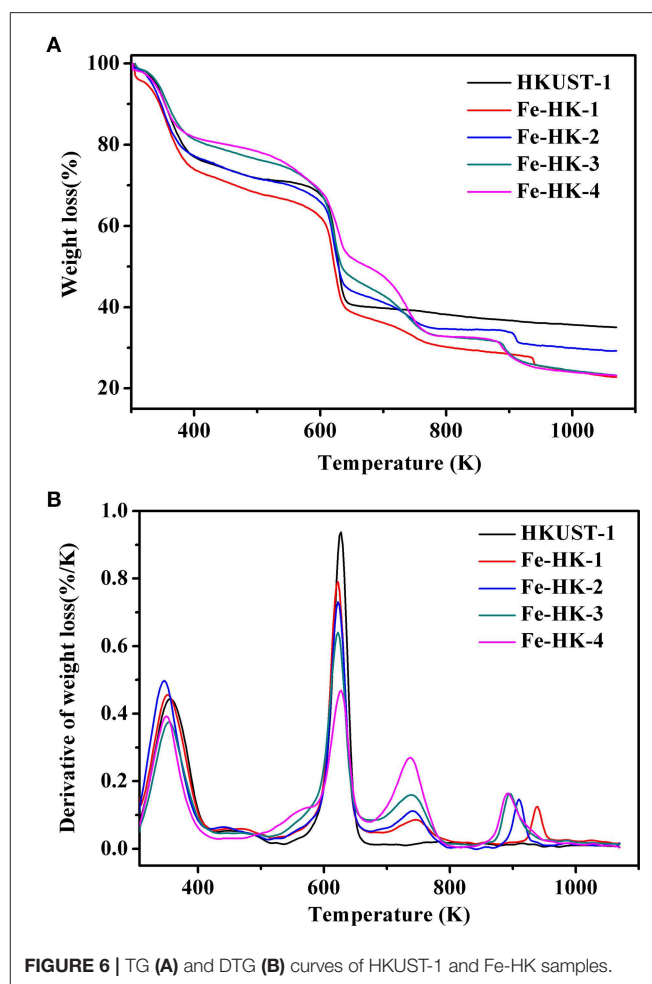
Figure 5 displays FTIR spectra of HKUST-1 and the Fe-HK samples. These FTIR spectra are nearly similar, which present





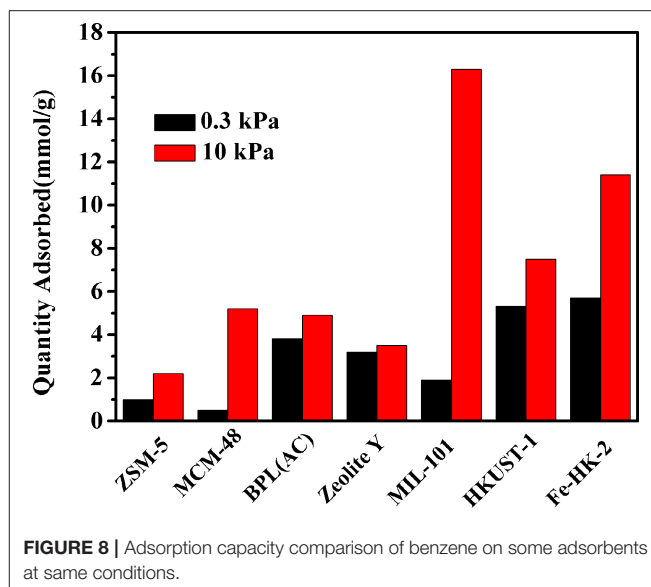
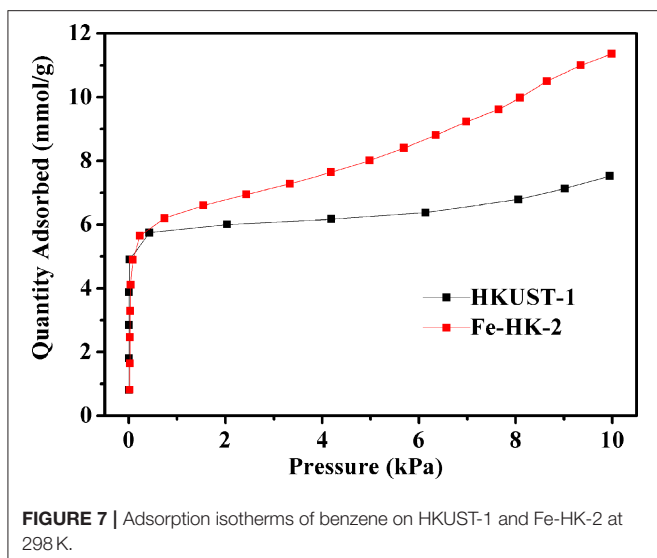
the asymmetric vibrations of carboxylate groups at 1,645/1,585 cm^{-1} and the symmetric vibrations at 1,445/1,373 cm^{-1} (Petit et al., 2012; Sun et al., 2015). However, it is noticed that for Fe-HK-3 and Fe-HK-4, the two bands at 1,645/1,585 cm^{-1} shift to lower wavenumbers, and a new band appears at 1,715 cm^{-1} belonged to the partially coordinated trimesic acid (Majano et al., 2014). Moreover, the band at 730 cm^{-1} is ascribed to the vibration of Cu-O, in which copper ions coordinate with the carboxylate groups of BTC (Lin et al., 2014). A new band appears at 711 cm^{-1} , which is ascribed to the vibration of Fe-O, indicating that iron ions coordinate with the carboxylate groups of BTC (Tan et al., 2015; Abdpour et al., 2018). The peak intensity at 711 cm^{-1} becomes stronger, while the peak intensity at 730 cm^{-1} becomes weaker as the increase of molar ratio of Fe/Cu.

Figure 6 exhibits TG and DTG curves of HKUST-1 and the Fe-HK samples. It is apparent that HKUST-1 and the Fe-HK samples present the different weight loss patterns. HKUST-1 exhibits two weight loss steps. The first weight loss below 373 K corresponds to the loss of guest molecules. The second weight loss between 523 and 673 K is assigned to the removal of BTC ligands coordinated to Cu^{2+} and the formation of CuO (Lin et al., 2012). Interestingly, all the Fe-HK samples exhibit four weight loss steps in **Figure 6B**. The first peak is similar to that of HKUST-1. The second peak broadens after the incorporation of Fe^{3+} ions. Thus, the second weight loss of the Fe-HK samples can correspond to the decomposition of organic ligands linked to Cu^{2+} and Fe^{3+} ions to form CuO and Fe_3O_4 at the same time (Petit and Bandoz, 2012). Additionally, a new peak as the third weight loss reveals between 673 and 800 K, which is ascribed to the reduction of $\text{Fe}_3\text{O}_4\text{-Fe}_2\text{O}_3$ (Petit and Bandoz, 2012). Another new peak as the fourth weight loss occurs between 800 and 1,000 K, which is due to the reduction of Fe_2O_3 to FeO (Petit and Bandoz, 2012).



Adsorption Isotherms of Benzene

Figure 7 presents adsorption isotherms of benzene on HKUST-1 and the optimal sample Fe-HK-2 at 298 K. It is observed that benzene adsorption capacities of HKUST-1 and Fe-HK-2 exhibit a sharp rise at low pressure (<0.5 kPa), which is ascribed to the micropore adsorption owing to the metal- π interactions between benzene molecules and the metal cations as well as the π - π stacking and electrostatic interactions between benzene molecules and the organic ligand (Sun et al., 2017). Subsequently, benzene adsorption capacity of HKUST-1 reaches a plateau followed by a slight increase at 8 kPa, which is related to the intermolecular π - π interactions of benzene (Zhu et al., 2017). Nevertheless, benzene adsorption capacity of Fe-HK-2 presents a gradual increase at high pressure, which is mainly attributed to the mesopore filling due to the π - π and electrostatic interactions between benzene molecules and the organic ligand as well as the intermolecular benzene-benzene interactions (Sun et al., 2017). Moreover, the Fe-HK sample exhibits higher saturated adsorption capacity of benzene than HKUST-1. The maximum adsorption capacity of benzene on Fe-HK-2 is up to 11.4 mmol/g, which is 1.5 times higher than that on HKUST-1 (7.5 mmol/g). The great increase in benzene capacity of Fe-HK-2 can be



attributed to its higher BET surface area and pore volume than HKUST-1.

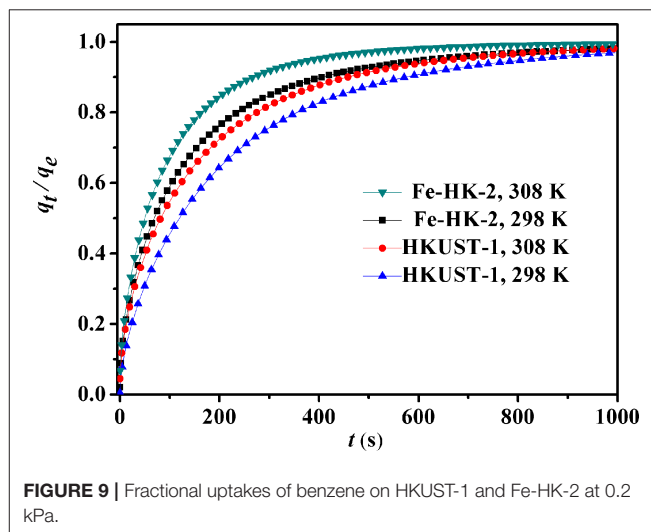
For comparison, the adsorption capacities of benzene on some typical porous materials at 0.3 and 10 kPa are shown in **Figure 8**. It indicates that the synthesized HKUST-1 and Fe-HK-2 possess much higher benzene capacities than the conventional adsorbents, e.g., ZSM-5 (Jhung et al., 2007), MCM-48 (Hartmann and Bischof, 1999), BPL(AC) (Zhao et al., 1998) and Zeolite Y (Zhao et al., 1998). It is also seen that the uptake of benzene on Fe-HK-2 at high pressure 10 kPa is lower than some MOFs [i.e., MIL-101 (Sun et al., 2017)], whereas, the benzene adsorption capacity of 5.7 mmol/g on the Fe-HK-2 at low pressure 0.3 kPa is 3 times larger than that of MIL-101 (1.9 mmol/g). One reason might be that Fe-HK-2 with smaller micropore size is favored for benzene adsorption at low pressure in comparison with MIL-101. Therefore, the hierarchical Fe-HK-2 exhibits certain advantages over some conventional adsorbents or MOFs.

Adsorption Kinetics of Benzene

Figure 9 shows the kinetic curves of benzene on HKUST-1 and Fe-HK-2 at 298 and 308 K. Compared to HKUST-1, equilibrium uptakes of benzene on Fe-HK-2 are achieved in a shorter time owing to the presence of mesopores. In order to obtain the intracrystalline diffusion coefficient of benzene on HKUST-1 and Fe-HK-2, the plots of fractional uptake (q_t/q_e) of benzene vs. the square root of adsorption time at 298 and 308 K are presented in **Figure 10**. The diffusion time constants (D_M/r_c^2 , s^{-1}) were obtained from the slope of q_t/q_e vs. \sqrt{t} based on the diffusion model (Equation 1) (Sui et al., 2013; Zhu et al., 2017). Their activation energy (E_a) was estimated by Arrhenius equation (Equation 2) (Hu et al., 2018).

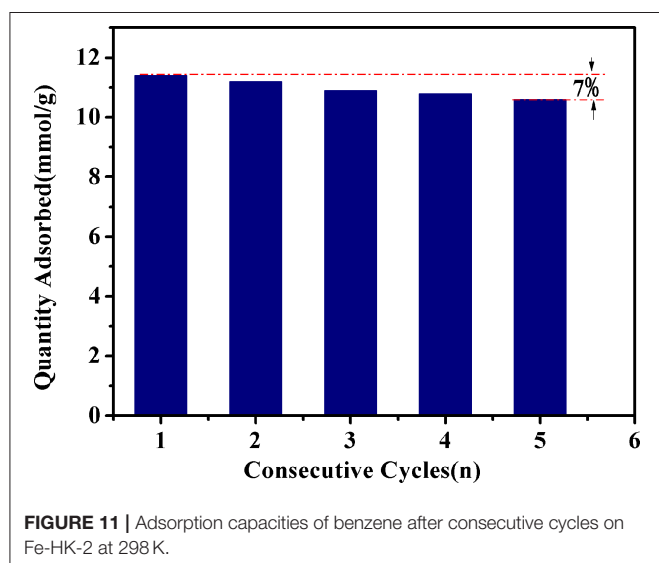
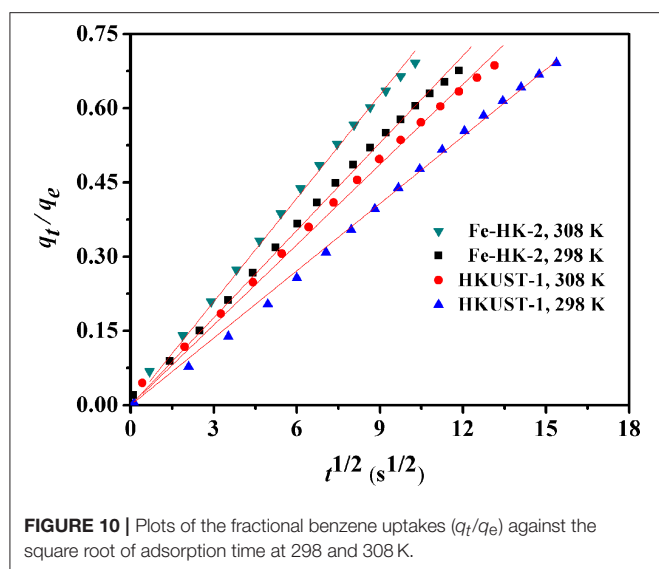
$$\frac{q_t}{q_e} \cong \frac{6}{r_c} \sqrt{\frac{D_M t}{\pi}} \quad (1)$$

$$\ln D_M = \ln A - \frac{E_a}{RT} \quad (2)$$



where q_e (mg/g) and q_t (mg/g) are the uptakes of benzene on adsorbent per gram at equilibrium and time t , D_M (cm^2/s) is the intracrystalline diffusion coefficient, r_c (cm) is the crystal radius, R is the gas constant and A is the Arrhenius factor.

Table S2 lists benzene diffusivity parameters and the activation energies of HKUST-1 and Fe-HK-2. The high regression coefficients ($R^2 > 0.996$) suggests that the diffusion model can fit the kinetic curves of benzene well. The diffusion time constants (D_M/r_c^2) of benzene on the HKUST-1 and Fe-HK-2 are in the range of $(1.78-2.54) \times 10^{-4}$ and $(3.02-4.23) \times 10^{-4} s^{-1}$, respectively. Corresponding diffusion coefficients (D_M) using the average particle radius r_c of $4 \mu m$ (**Figure S1**) are $(2.85-4.07) \times 10^{-11}$ and $(4.83-6.76) \times 10^{-11} cm^2/s$ for HKUST-1 and Fe-HK-2, respectively. The diffusivity value of Fe-HK-2 is 1.7 times faster than that of parent HKUST-1. It is also noticed from **Table S2** that the activation energy E_a for diffusion of benzene on



Fe-HK-2 is about 25.78 kJ/mol, which is smaller than that on HKUST-1 owing to faster benzene diffusion on Fe-HK-2. These results indicate that the Fe-HK-2 with mesopores exhibits the enhanced diffusion and mass transport than HKUST-1.

Recycling Performance of Fe-HK-2 for Benzene Adsorption

The reversibility of Fe-HK-2 for benzene adsorption was also tested in this work. Adsorption was measured at 10 kPa, then desorption was performed at 373 K under high vacuum. **Figure 11** presents adsorption capacities of benzene after consecutive cycles on Fe-HK-2 at 298 K. After five consecutive cycles, the adsorption capacities of

benzene on Fe-HK-2 decreases by only 7%, indicating that the Fe-HK-2 possesses an outstanding reversibility of VOCs adsorption.

CONCLUSIONS

In summary, we proposed a facile strategy to prepare novel hierarchical Fe(III)-doped Cu-MOF materials with enhanced benzene adsorption. The characterizations showed that the introduction of Fe^{3+} ions could form new mesopores in Fe-HK. The hierarchical-pore Fe-HK-2 exhibited high BET surface area of 1,707 m^2/g , mesopore volume of 0.31 cm^3/g and total pore volume of 0.93 cm^3/g , which are much higher than those of the original HKUST-1. This improves benzene adsorption capacity of Fe-HK-2, showing 1.5 times greater than that on HKUST-1. Fe-HK-2 also exhibited faster diffusivity and excellent reversibility of benzene adsorption. Thus, the hierarchical-pore Fe-HK-2 could be a promising adsorbent for VOCs adsorption. The results also indicate that metal ion doping can be a facile strategy to synthesize hierarchical-pore MOFs with enhanced adsorption performance.

DATA AVAILABILITY STATEMENT

The datasets generated for this study are available on request to the corresponding author.

AUTHOR CONTRIBUTIONS

XS, XG, WX, and W-JC have provided substantial contribution to the acquisition, interpretation and analysis of data, as well as to the drafting of the work. QX, XP, XZ, YL, and Q-HW performed essential work regarding to the conception and design of the research presented and to its critical revision for important intellectual content. They all approve the version to be published and agree to be accountable to investigate and resolve any question related to the accuracy or integrity of any part of the work.

FUNDING

This work was supported by the National Natural Science Foundation of China (Nos. 21606144, 21878101), the Program for the Cultivation of Outstanding Young Scientific Talents in Fujian Province University, the Natural Science Foundation of Fujian Province (No. 2017J05026), and Quanzhou City Science & Technology Program of China (Nos. 2017G022, 2017Z028, and 2018C127R).

SUPPLEMENTARY MATERIAL

The Supplementary Material for this article can be found online at: <https://www.frontiersin.org/articles/10.3389/fchem.2019.00652/full#supplementary-material>

REFERENCES

- Abdour, S., Kowsari, E., Moghaddam, M. R. A., Schmolke, L., and Janiak, C. (2018). MIL-100 (Fe) nanoparticles supported on urchin like Bi₂S₃ structure for improving photocatalytic degradation of rhodamine-B dye under visible light irradiation. *J. Solid State Chem.* 266, 54–62. doi: 10.1016/j.jssc.2018.07.006
- Ahmed, I., and Jung, S. H. (2016). Remarkable adsorptive removal of nitrogen-containing compounds from a model fuel by a graphene oxide/MIL-101 composite through a combined effect of improved porosity and hydrogen bonding. *J. Hazard. Mater.* 314, 318–325. doi: 10.1016/j.jhazmat.2016.04.041
- Bradshaw, D., El-Hankari, S., and Lupica-Spannolò, L. (2014). Supramolecular templating of hierarchically porous metal-organic frameworks. *Chem. Soc. Rev.* 43, 5431–5443. doi: 10.1039/C4CS00127C
- Chen, X., Jiang, X., Yin, C., Zhang, B., and Zhang, Q. (2019). Facile fabrication of hierarchically porous ZIF-8 for enhanced adsorption of antibiotics. *J. Hazard. Mater.* 367, 194–204. doi: 10.1016/j.jhazmat.2018.12.080
- Chuah, C. Y., Goh, K., and Bae, T. H. (2017). Hierarchically structured HKUST-1 nanocrystals for enhanced SF₆ capture and recovery. *J. Phys. Chem.* 121, 6748–6755. doi: 10.1021/acs.jpcc.7b00291
- Duan, C., Li, F., Li, L., Zhang, H., Wang, X., Xiao, J., et al. (2018a). Hierarchically structured metal-organic frameworks assembled by hydroxy double salt-temple synergy with high space-time yields. *CrystEngComm* 20, 1057–1064. doi: 10.1039/C7CE01843F
- Duan, C., Li, F., Luo, S., Xiao, J., Li, L., and Xi, H. (2018b). Facile synthesis of hierarchical porous metal-organic frameworks with enhanced catalytic activity. *Chem. Eng. J.* 334, 1477–1483. doi: 10.1016/j.cej.2017.11.086
- Duan, C., Zhang, H., Peng, A., Li, F., Xiao, J., Zou, J., et al. (2018c). Synthesis of hierarchically structured metal-organic frameworks by a dual-functional surfactant. *Chem. Select.* 3, 5313–5320. doi: 10.1002/slct.201800571
- Duan, L. H., Dong, X. Y., Wu, Y. Y., Li, H. L., Wang, L., and Song, L. J. (2013). Adsorption and diffusion properties of xylene isomers and ethylbenzene in metal-organic framework MIL-53(Al). *J. Porous Mat.* 20, 431–440. doi: 10.1007/s10934-012-9612-z
- Ebrahim, A. M., and Bandosz, T. J. (2013). Ce(III) doped Zr-based MOFs as excellent NO₂ adsorbents at ambient conditions. *ACS Appl. Mater. Inter.* 5, 10565–10573. doi: 10.1021/am402305u
- Hartmann, M., and Bischof, C. (1999). Mechanical stability of mesoporous molecular sieve MCM-48 studied by adsorption of benzene, n-heptane, and cyclohexane. *J. Phys. Chem.* 103, 6230–6235. doi: 10.1021/jp991103a
- He, S., Chen, Y., Zhang, Z., Ni, B., He, W., and Wang, X. (2016). Competitive coordination strategy for the synthesis of hierarchical-pore metal-organic framework nanostructures. *Chem. Sci.* 7, 7101–7105. doi: 10.1039/C6SC02272C
- Horcajada, P., Chevreau, H., Heurtaux, D., Benyettou, F., Salles, F., Devic, T., et al. (2014). Extended and functionalized porous iron(III) tri- or dicarboxylates with MIL-100/101 topologies. *Chem. Commun.* 50, 6872–6874. doi: 10.1039/c4cc02175d
- Hu, P., Liang, X., Yaseen, M., Sun, X., Tong, Z., Zhao, Z., et al. (2018). Preparation of highly-hydrophobic novel N-coordinated UiO-66 (Zr) with dopamine via fast mechano-chemical method for (CHO-/Cl-)-VOCs competitive adsorption in humid environment. *Chem. Eng. J.* 332, 608–618. doi: 10.1016/j.cej.2017.09.115
- Huang, H., Li, J. R., Wang, K., Han, T., Tong, M., Li, L., et al. (2015). An *in situ* self-assembly template strategy for the preparation of hierarchical-pore metal-organic frameworks. *Nat. Commun.* 6:8847. doi: 10.1038/ncomms9847
- Jhung, S. H., Lee, J. H., Yoon, J. W., Serre, C., Férey, G., and Chang, J. S. (2007). Microwave synthesis of chromium terephthalate MIL-101 and its benzene sorption ability. *Adv. Mater.* 19, 121–124. doi: 10.1002/adma.200601604
- Li, H., Wang, K., Sun, Y., Lollar, C. T., Li, J., and Zhou, H. C. (2018). Recent advances in gas storage and separation using metal-organic frameworks. *Mater. Today* 21, 108–121. doi: 10.1016/j.mattod.2017.07.006
- Lin, K. S., Adhikari, A. K., Ku, C. N., Chiang, C. L., and Kuo, H. (2012). Synthesis and characterization of porous HKUST-1 metal organic frameworks for hydrogen storage. *Int. J. Hydrogen Energ.* 37, 13865–13871. doi: 10.1016/j.ijhydene.2012.04.105
- Lin, R. B., Li, L. B., Zhou, H. L., Wu, H., He, C. H., Li, S., et al. (2018). Molecular sieving of ethylene from ethane using a rigid metal-organic framework. *Nat. Mater.* 17, 1128–1133. doi: 10.1038/s41563-018-0206-2
- Lin, S., Song, Z., Che, G., Ren, A., Li, P., Liu, C., et al. (2014). Adsorption behavior of metal-organic frameworks for methylene blue from aqueous solution. *Micropor. Mesopor. Mat.* 193, 27–34. doi: 10.1016/j.micromeso.2014.03.004
- Lv, D., Chen, Y., Li, Y., Shi, R., Wu, H., Sun, X., et al. (2017). Efficient mechanochemical synthesis of MOF-5 for linear alkanes adsorption. *J. Chem. Eng. Data* 62, 2030–2036. doi: 10.1021/acs.jced.7b00049
- Majano, G., Martin, O., Hammes, M., Smeets, S., Baerlocher, C., and Perez-Ramirez, J. (2014). Solvent-mediated reconstruction of the metal-organic framework HKUST-1 (Cu₃(BTC)₂). *Adv. Funct. Mater.* 24, 3855–3865. doi: 10.1002/adfm.201303678
- Mao, Y., Chen, D., Hu, P., Guo, Y., Ying, Y., Ying, W., et al. (2015). Hierarchical mesoporous metal-organic frameworks for enhanced CO₂ capture. *Chem. Eur. J.* 21, 15127–15132. doi: 10.1002/chem.201502515
- Meng, X. H., Lin, C. H., Zhang, Y. H., Qin, H. B., Cao, S., and Duan, L. H. (2019). Mass transfer behavior of benzene in hierarchically structured ZSM-5. *Front. Chem.* 7:502. doi: 10.3389/fchem.2019.00502
- Petit, C., and Bandosz, T. J. (2012). Exploring the coordination chemistry of MOF-graphite oxide composites and their applications as adsorbents. *Dalton T.* 41, 4027–4035. doi: 10.1039/c2dt12017h
- Petit, C., Levasseur, B., Mendoza, B., and Bandosz, T. J. (2012). Reactive adsorption of acidic gases on MOF/graphite oxide composites. *Micropor. Mesopor. Mat.* 154, 107–112. doi: 10.1016/j.micromeso.2011.09.012
- Sui, H., Liu, J. J., He, L., Li, X. G., and Jani, A. (2019). Adsorption and desorption of binary mixture of acetone and ethyl acetate on silica gel. *Chem. Eng. Sci.* 197, 185–194. doi: 10.1016/j.ces.2018.12.010
- Sui, P. P., Meng, X. H., Wu, Y. Y., Zhao, Y. Y., Song, L. J., Sun, Z. L., et al. (2013). Adsorption and diffusion of benzene and thiophene over Y/MCM-41 composite zeolite. *Sci. Adv. Mater.* 5, 1132–1138. doi: 10.1166/sam.2013.1564
- Sun, X., Li, H., Li, Y., Xu, F., Xiao, J., Xia, Q., et al. (2015). A novel mechanochemical method for reconstructing the moisture-degraded HKUST-1. *Chem. Commun.* 51, 10835–10838. doi: 10.1039/C5CC02809D
- Sun, X., Lv, D., Chen, Y., Wu, Y., Wu, Q., Xia, Q., et al. (2017). Enhanced adsorption performance of aromatics on a novel chromium-based MIL-101@graphite oxide composite. *Energ. Fuel.* 31, 13985–13990. doi: 10.1021/acs.energyfuels.7b02665
- Sun, X. J., Li, Y. J., Xi, H. X., and Xia, Q. B. (2014). Adsorption performance of a MIL-101(Cr)/graphite oxide composite for a series of n-alkanes. *RSC Adv.* 4, 56216–56223. doi: 10.1039/C4RA08598A
- Tan, F., Liu, M., Li, K., Wang, Y., Wang, J., Guo, X., et al. (2015). Facile synthesis of size-controlled MIL-100 (Fe) with excellent adsorption capacity for methylene blue. *Chem. Eng. J.* 281, 360–367. doi: 10.1016/j.cej.2015.06.044
- Vellingiri, K., Kumar, P., Deep, A., and Kim, K. H. (2017). Metal-organic frameworks for the adsorption of gaseous toluene under ambient temperature and pressure. *Chem. Eng. J.* 307, 1116–1126. doi: 10.1016/j.cej.2016.09.012
- Vellingiri, K., Szulejko, J. E., Kumar, P., Kwon, E. E., Kim, K. H., Deep, A., et al. (2016). Metal organic frameworks as sorption media for volatile and semi-volatile organic compounds at ambient conditions. *Sci. Rep.* 6:27813. doi: 10.1038/srep27813
- Wang, D., Wu, G., Zhao, Y., Cui, L., Shin, C. H., Ryu, M. H., et al. (2018). Study on the copper(II)-doped MIL-101(Cr) and its performance in VOCs adsorption. *Environ. Sci. Pollut. R.* doi: 10.1007/s11356-018-2849-6
- Wu, Y., Liu, D., Chen, H., Qian, Y., Xi, H., and Xia, Q. (2015). Enhancement effect of lithium-doping functionalization on methanol adsorption in copper-based metal-organic framework. *Chem. Eng. Sci.* 123, 1–10. doi: 10.1016/j.ces.2014.10.010
- Xian, S., Yu, Y., Xiao, J., Zhang, Z., Xia, Q., Wang, H., et al. (2015). Competitive adsorption of water vapor with VOCs dichloroethane, ethyl acetate and benzene on MIL-101(Cr) in humid atmosphere. *RSC Adv.* 5, 1827–1834. doi: 10.1039/C4RA10463C
- Yang, X., Wu, S., Wang, P., and Yang, L. (2018). Hierarchical 3D ordered meso-/macroporous metal-organic framework produced through a facile template-free self-assembly. *J. Solid State Chem.* 258, 220–224. doi: 10.1016/j.jssc.2017.10.020
- Yuan, S., Zou, L., Qin, J. S., Li, J., Huang, L., Feng, L., et al. (2017). Construction of hierarchically porous metal-organic frameworks through linker labilization. *Nat. Commun.* 8:15356. doi: 10.1038/ncomms15356
- Zhang, X. D., Yang, Y., Lv, X. T., Wang, Y. X., Liu, N., Chen, D., et al. (2019). Adsorption/desorption kinetics and breakthrough of gaseous toluene

- for modified microporous-mesoporous UiO-66 metal organic framework. *J. Hazard. Mater.* 366, 140–150. doi: 10.1016/j.jhazmat.2018.11.099
- Zhang, X. Y., Gao, B., Creamer, A. E., Cao, C. C., and Li, Y. C. (2017). Adsorption of VOCs onto engineered carbon materials: a review. *J. Hazard. Mater.* 338, 102–123. doi: 10.1016/j.jhazmat.2017.05.013
- Zhao, X., Ma, Q., and Lu, G. (1998). VOC removal: comparison of MCM-41 with hydrophobic zeolites and activated carbon. *Energ. Fuel.* 12, 1051–1054. doi: 10.1021/ef980113s
- Zhao, Z. X., Wang, S., Yang, Y., Li, X. M., Li, J., and Li, Z. (2015). Competitive adsorption and selectivity of benzene and water vapor on the microporous metal organic frameworks (HKUST-1). *Chem. Eng. J.* 259, 79–89. doi: 10.1016/j.cej.2014.08.012
- Zhou, Z., Mei, L., Ma, C., Xu, F., Xiao, J., Xia, Q., et al. (2016). A novel bimetallic MIL-101(Cr, Mg) with high CO₂ adsorption capacity and CO₂/N₂ selectivity. *Chem. Eng. Sci.* 147, 109–117. doi: 10.1016/j.ces.2016.03.035
- Zhu, M., Hu, P., Tong, Z., Zhao, Z., and Zhao, Z. (2017). Enhanced hydrophobic MIL (Cr) metal-organic framework with high capacity and selectivity for benzene VOCs capture from high humid air. *Chem. Eng. J.* 313, 1122–1131. doi: 10.1016/j.cej.2016.11.008
- Zhu, M., Tong, Z., Zhao, Z., Jiang, Y., and Zhao, Z. (2016). A microporous graphitized biocarbon with high adsorption capacity toward benzene volatile organic compounds (VOCs) from humid air at ultralow pressures. *Ind. Eng. Chem. Res.* 55, 3765–3774. doi: 10.1021/acs.iecr.6b00056
- Zhu, T., Zhang, X., Han, Y., Liu, T., Wang, B., and Zhang, Z. (2019). Preparation of zeolite X by the aluminum residue from coal fly ash for the adsorption of volatile organic compounds. *Front. Chem.* 7:341. doi: 10.3389/fchem.2019.00341

Conflict of Interest: The authors declare that the research was conducted in the absence of any commercial or financial relationships that could be construed as a potential conflict of interest.

Copyright © 2019 Sun, Gu, Xu, Chen, Xia, Pan, Zhao, Li and Wu. This is an open-access article distributed under the terms of the Creative Commons Attribution License (CC BY). The use, distribution or reproduction in other forums is permitted, provided the original author(s) and the copyright owner(s) are credited and that the original publication in this journal is cited, in accordance with accepted academic practice. No use, distribution or reproduction is permitted which does not comply with these terms.